Uptake Dynamics and Diffusion of HCl in Sulfuric Acid Solution Measured in Single Levitated Microdroplets

M. Schwell[†] and H. Baumgärtel

Institut für Physikalische und Theoretische Chemie, Freie Universität Berlin, Takustrasse 3, 14195 Berlin, Germany

I. Weidinger,[‡] B. Krämer, H. Vortisch, L. Wöste, and T. Leisner*

Institut für Experimentalphysik, Freie Universität Berlin, Arnimalle 14, D-14195 Berlin, Germany

E. Rühl

Fachbereich Physik, Universität Osnabrück, Barbarastrasse 7, D-49069 Osnabrück, Germany

Received: November 30, 1999; In Final Form: April 17, 2000

The uptake dynamics of HCl by single sulfuric acid microdroplets under stratospheric conditions is investigated. The droplets are typically 30−70 μm in diameter and weakly charged so that they can be stored in an electrodynamic trap. The gas uptake of the droplets is monitored either by measuring their size by angle resolved Mie- scattering patterns or by electrostatic balancing of the droplets in the trap. At low temperatures and high sulfuric acid concentration (T < 190 K for 48 wt % H_2SO_4 and T < 195 K for 56 wt % H_2SO_4, respectively), liquid-phase diffusion inside the droplet is the rate-limiting step in the overall uptake process. In this regime, the diffusion coefficients D^{liq} of HCl in supercooled sulfuric acid solutions are found to increase strongly with temperature and H_2O concentration. The results are discussed with respect to diffusion models that have been proposed recently. In contrast, at higher temperatures and lower sulfuric acid concentrations (30−40 wt % H_2SO_4, 185−207 K) gas-phase diffusion with subsequent accommodation/dissolution at the liquid surface determines the observed uptake velocity. A new method to deduce accommodation coefficients α is proposed.

I. Introduction

Hydrogen chloride is a stratospheric trace gas that plays a key role in the heterogeneous chlorine chemistry of polar stratospheric clouds (PSC). PSCs are considered to be responsible for the temporal destruction of the Antarctic polar ozone layer in springtime via chlorine activation.[1] It is now well established that stratospheric chlorine is efficiently stored in the reservoir species HCl and $ClONO_2$. This compound can be activated via the reactions 1−3 (for a review on PSC chemistry see for example ref 2).

$$ClONO_2 + HCl \xrightarrow{\text{particle}} Cl_2 + HNO_3 \quad (1)$$

$$ClONO_2 + H_2O \xrightarrow{\text{particle}} HOCl + HNO_3 \quad (2)$$

$$HOCl + HCl \xrightarrow{\text{particle}} Cl_2 + H_2O \quad (3)$$

The reactions take place either on the surface or in the bulk of stratospheric particles. These are mainly background aerosols, consisting of supercooled liquid sulfuric acid, and PSCs which are formed at T < 195 K. The rates of the reactions 1−3 depend on the substrate and its microphysical state.[3] The resulting products are Cl_2 and HOCl, which are rapidly photolyzed after sunrise in polar spring. The photolysis yields efficiently atomic chlorine which subsequently triggers catalytic ozone destruction cycles.[4]

It was pointed out recently[2] that conditions with incomplete chlorine activation on a mesoscale (see for example ref 5) require the exact knowledge of reaction rates in order to model the chemical processes occurring in stratospheric particles. However, crucial parameters such as liquid diffusion and accommodation coefficients are still difficult to measure with standard laboratory approaches at stratospheric temperatures.[6−10]

The first step of the heterogeneous reactions 1 and 3 is the uptake of HCl by the particles. In this paper, we present results from a detailed study of the HCl uptake by supercooled sulfuric acid solution droplets using the technique of electrodynamic particle levitation. This method has become a powerful approach for investigations on physicochemical properties of aerosol particles (for a recent review see ref 11). The use of levitated particles avoids possible influences from the walls of the recipient or substrates. This is of special advantage if supercooled or supersaturated solutions are investigated. Additionally, this approach allows to quantify the uptake dynamics of gas-phase molecules into the liquid phase by monitoring the time-dependent optical properties of the levitated particle. In contrast, previous work made use of Knudsen cells,[8] droplet trains,[9] and coated flow tubes,[10] where the HCl uptake was monitored as a depletion of the reactant in the gas phase. Hence, in these

* To whom correspondence should be addressed. Electronic mail: leisner@physik.fu-berlin.de

[†] Present address: DAMAp Observatoire de Paris-Meudon, UMR 8588 du CNRS, 5 place Jules Jannsen, F-92195 Meudon Cedex, France.

[‡] Present address: Institut für Physikalische und Theoretische Chemie, Freie Universität Berlin, Takustrasse 3, 14195 Berlin, Germany.

10.1021/jp994200c CCC: $19.00
Published on Web 07/01/2000

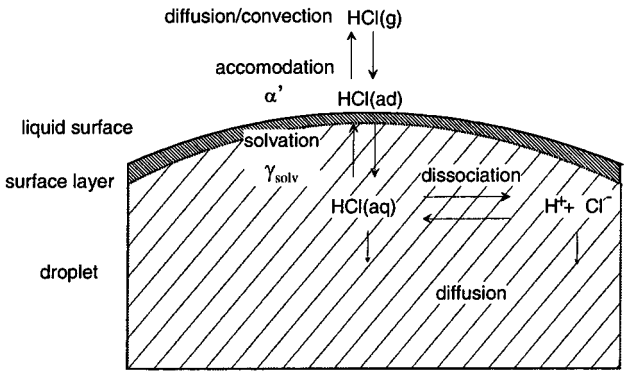

Figure 1. Relevant transport processes for the gas uptake of a liquid droplet.

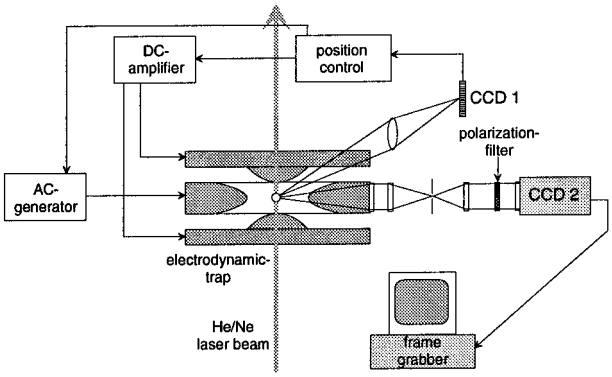

Figure 2. Optical and electrical setup of the droplet trap.

experiments wall effects are more difficult to exclude. Various processes that are involved in the uptake of a gas-phase molecule into the liquid phase are illustrated in Figure 1. After being transported toward the droplet, the molecule becomes accommodated on the surface. This process may be described by a mass accommodation coefficient α' being the fraction of "sticking molecules", while 1-α' is the fraction of molecules being reflected to the gas phase after impinging on the surface. The subsequent fate of an adsorbed molecule is either solvation or desorption. The kinetics of the former process may be summarized by the solvation coefficient γ_{solv}. The overall phase passage behavior of the entering molecules is described by the accommodation coefficient α, which corresponds to the product of the coefficient α' and γ_{solv}. Finally, the solvated molecule diffuses in the liquid bulk.

In principle, light scattering experiments on single levitated particles allow to distinguish between these subsequent steps. In this paper we quantify liquid diffusion coefficients D^{liq} of HCl in supercooled H_2SO_4 solutions and propose a method to measure accommodation coefficients. The measured D^{liq} are compared to various diffusion models (for a survey see ref 12).

II. Experiment

The experimental setup has been described earlier in detail.[13] Briefly, it consists of a standard electrodynamic trap with hyperbolic electrodes.[14] Figure 2 shows a schematic view of the trap together with the components that are used for positioning of the droplets and detection of elastic light scattering. The microdroplet is illuminated by a linearly polarized helium/neon laser operating at $\lambda = 632.8$ nm. Angle-resolved light-scattering of the droplet is recorded using a CCD camera. Two polarization filters are located right in front of the camera such that the light polarized parallel to the scattering plane is imaged on the lower part, whereas the perpendicular

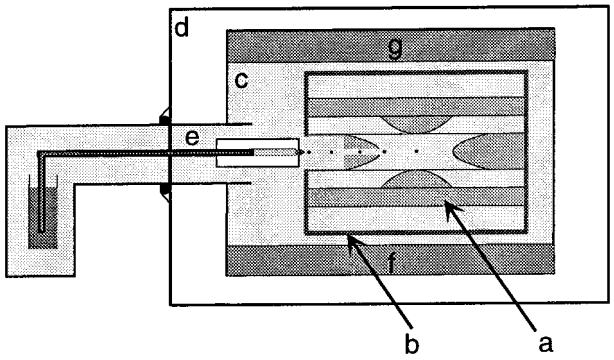

Figure 3. Schematic view of the trap assembly: (a) electrodynamic trap, (b) copper enclosure, (c) climate chamber, (d) insulation chamber, (e) heated droplet injector, (f) cooled bottom flange, (g) cooled top flange.

polarized light is imaged on the upper part of the CCD camera. The elastic light scattering patterns are digitized with a programmable frame grabber as indicated in Figure 2.

The vertical position of the droplet is permanently monitored by a CCD line in order to keep growing or evaporating droplets constantly at the same location. This is accomplished by adjusting a DC voltage U_{DC} that is applied to the end-cap electrodes of the trap. This voltage compensates the gravitational force on the droplet and is related to its mass-to-charge ratio m/q as

$$\frac{m}{q} = \frac{bU_{DC}}{gz_0} \tag{4}$$

Here, g is the acceleration of gravity, z_0 is the distance between the end-cap electrodes, and b is a factor that accounts for their nonplanar geometry. The m/q value is also used to adjust permanently the AC voltage of the ring-shaped electrode according to the stability conditions for levitation.

To realize stratospheric conditions, the trap is mounted inside a climate chamber. A schematic view of the setup is given in Figure 3. The trap (Figure 3a) is enclosed inside a copper housing (Figure 3b) which ensures a homogeneous temperature profile across the trap. The trap assembly is located inside the climate chamber (Figure 3c), where the atmospheric compositions and temperatures of interest are realized. A vacuum vessel (Figure 3d) provides thermal insulation for the whole setup.

Within the climate chamber, a temperature gradient is maintained by applying a higher cooling power to the bottom flange (Figure 3f) than to the top flange (Figure 3g) of the chamber. The water partial pressure inside the trap is then given by the vapor pressure of ice at the temperature of the bottom flange. This allows to control the humidity inside the trap independently from the trap temperature. If the temperature gradient is zero, the relative humidity (RH) in the trap with respect to ice is 100%, whereas large temperature gradients correspond to low RH. The temperature of the trap adjusts itself roughly at the average between the temperatures at (f) and (g) and is continuously monitored with a precision of about ± 0.2 K.

Single sulfuric acid solution droplets are injected directly into the cold atmosphere using a modified version of a commercially available piezo-driven droplet generator (Figure 3e). The droplet temperature equilibrates instantaneously with the temperature within the trap chamber. The time scales of this process are estimated to be of the order of a few milliseconds.[13,15,16]

The gas phase of the climate-chamber leaks through a 20 μm nozzle into the evacuated outer chamber yielding there a

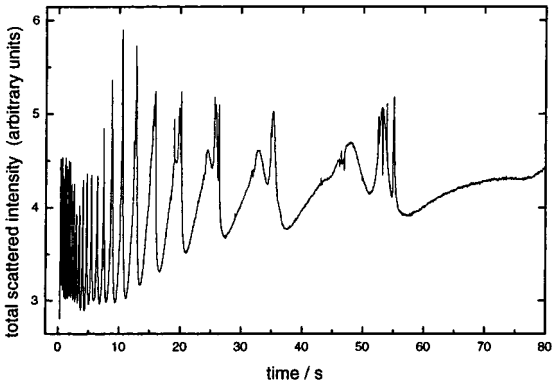

Figure 4. Total light scattering intensity from a 48 wt % sulfuric acid droplet during the HCl uptake.

pressure of approximately 10^{-4} mbar. The nozzle is located near the ionization region of a quadrupole mass spectrometer (QMS, Stanford RGA 200) which records the relative composition of the atmosphere of the trap chamber.

A N_2/HCl mixture (0.1−1% HCl) is prepared manometrically by using calibrated piezo-resistive capacitor instruments (Kistler). It is admitted to the trap chamber at a total pressure of 200 mbar, which corresponds to an HCl partial pressure between 10^{-4} and 10^{-5} bar. The flow through the inner chamber is controlled by a servo driven valve. It has to be kept very low (5−10 cm^3/s) in order to keep the droplets position undisturbed during the gas uptake experiments. However, under these conditions the HCl^+ mass signal of the QMS ($m/z = 36$) of the same gas mixture is lower than under high flow conditions, where it is calibrated. This indicates that HCl entering the trap chamber is partially adsorbed on the walls of the recipient and the Paul trap. The consequences of this uncertainty in the HCl partial pressure will be addressed in the following section.

When HCl is present in the gas phase, the injected droplet starts growing instantaneously until it saturates with HCl. The diameter *d*, the mass *m*, and the refractive index *n* of the droplet can be determined during the uptake process by three alternative methods:

(i) The experimentally recorded, angular-resolved patterns of elastically scattered light are fitted using Mie theory.[17] This procedure is described in refs 13 and 18. It yields the diameter and index of refraction of the droplet as a function of time. However, this procedure is time-consuming when it is applied to the evaluation of each camera frame since they are recorded at a repetition rate of 25 Hz. Furthermore, experimental conditions at low temperatures are not always stable enough to evaluate the angular resolved scattering patterns with sufficient precision.

(ii) A faster way to measure the HCl uptake is the evaluation of the morphology-dependent resonances (MDRs). These sharp maxima in light scattering occur upon illumination with a constant wavelength when a droplet changes its diameter and/or its refractive index (cf. Figure 4). In the cases of HCl uptake by sulfuric acid solutions, one expects that both the refractive index and the diameter will change. The occurrence of an MDR corresponds to a constant change in diameter, if the index of refraction *n* is constant or changes linearly with the droplet diameter. The absolute change in diameter can be obtained by evaluating angular resolved scattering patterns using the full Mie analysis (see above). However, during the uptake process, the concentration of HCl within droplet is no longer homogeneous, leading to a time-dependent and non-uniform index of refraction.

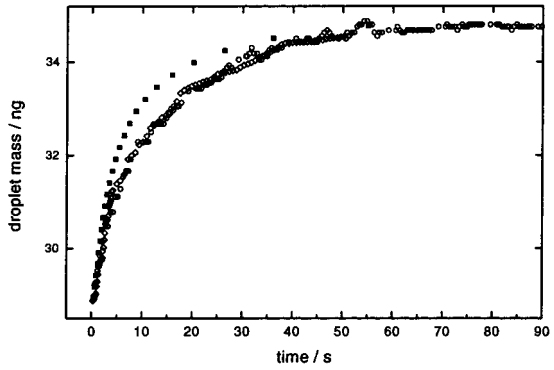

Figure 5. Comparison of uptake curves obtained from three different experimental methods: (i) hollow diamonds, analysis of the angular distribution of the scattered light; (ii) hollow circles, balance voltage measurements; (iii) full squares, values from the analysis of MDRs. For details see text.

(iii) The DC voltage U_{DC} that is applied to the end-caps of the Paul trap is a linear function of the droplet mass (eq 4) and provides an independent measure of the relative mass change of the droplet during the gas uptake. This method, however, requires a high stability of the droplet position in the center of the trap, a condition which is not always fulfilled at low temperature, reduced pressure, and high gas flux.

The three methods outlined above are compared in Figure 5. The data were recorded during the HCl uptake of a sulfuric acid droplet that contained initially 48 wt % H_2SO_4. The analysis of the angular resolved scattering patterns corresponds to the hollow diamonds, assuming constant density during the gas uptake. The validity of this assumption is evidenced by the good agreement with the curve that is obtained from U_{DC} measurements (hollow circles in Figure 5). The solid squares show the uptake curve calculated from MDR analysis, assuming a constant change in diameter between the resonances. Figure 5 indicates that this approach leads to an uptake velocity which is too large compared to the other methods. This is likely an indication for the fact that the refractive index does not change in a linear way with time. Nevertheless, we use this method in our data evaluation since it does not require a stable droplet position. The diffusion coefficients obtained from the analysis of MDRs have then be corrected by an empirical factor of 0.6. These are believed to be accurate within 30%.

The influence of the droplet charge on the uptake kinetics is investigated by varying the amount and polarity of the droplet charge within 1 order of magnitude. It is assumed that all excess charges are located on the surface so that possible influences on gas/liquid interactions may be anticipated. However, no influence on the HCl uptake velocity is found, even if the polarity of the droplet charge is inverted. Especially the latter finding leads to the conclusion that the surface charge density does not affect the gas/liquid interaction within the experimental error limits.

The observed changes in diameter and refractive index can be attributed to HCl uptake only when other processes, such as the uptake or evaporation of water, appear on a much longer time scale. As the gas-phase diffusion coefficients are similar for H_2O and HCl, this implies that the partial pressure of water has to be kept far below the partial pressure of HCl. We therefore operated the trap at low humidity by applying a large temperature gradient across the climate chamber, as discussed above. Under these conditions, sulfuric acid droplets in an inert atmosphere reach an equilibrium concentration of about 70 wt % within about 1 h. This corresponds to a water partial pressure in the chamber below 10^{-7} bar. The uptake experiments were

then performed at an HCl partial pressure of about 10^{-5} bar to ensure that HCl uptake is the dominant channel for the mass change of the droplets.

III. Results and Discussion

A. Uptake Dynamics. Figure 1 indicates that the transport processes that occur during the gas uptake can be divided into three steps: (i) diffusion through the gas phase, (ii) phase passage at the droplet surface (accommodation and solvation), and (iii) liquid diffusion inside the droplet. The slowest of these transport processes forms a bottleneck for the HCl uptake and limits the growth rate of the droplet. The first two steps of the uptake, i.e., gas-phase diffusion and surface hindrance, may be described by eq 5:[2,19]

$$\frac{\mathrm{d}n_{\mathrm{HCl}}^{\mathrm{liq}}}{\mathrm{d}t} = \frac{3D_{\mathrm{HCl}}^{*}}{kTr_0^2}(p_{\mathrm{HCl}}^{\infty} - p_{\mathrm{HCl}}^{\mathrm{vap}}) \tag{5}$$

with

$$D_{\mathrm{HCl}}^{*} = D_{\mathrm{HCl}}^{\mathrm{gas}}/(1 + 4D_{\mathrm{HCl}}^{\mathrm{gas}}/\alpha\, \bar{v}_{\mathrm{HCl}}\, r_0) \tag{6}$$

Here $\mathrm{d}n_{\mathrm{HCl}}^{\mathrm{liq}}/\mathrm{d}t$ denotes the growth rate in terms of the molecular number density of HCl inside the droplet and r_0 is the initial droplet radius. D_{HCl}^{*} is an "effective diffusion constant" introduced in refs 2 and 20. It comprises gas-phase diffusion and the phase passage. $D_{\mathrm{HCl}}^{\mathrm{gas}}$ (eq 6) is the diffusion coefficient of HCl in the gas phase. The term $p_{\mathrm{HCl}}^{\infty}$ is the HCl partial pressure at infinite distance from the droplet and $p_{\mathrm{HCl}}^{\mathrm{vap}}$ the HCl vapor pressure of the droplet which depends on the amount of HCl that is already dissolved. Finally $\bar{v}_{\mathrm{HCl}}$ is the mean thermal velocity of the HCl in the gas phase.

Equations 5 and 6 can be derived by combining Fick's 2nd law of diffusion and the Hertz−Knudsen equation.[21] It is valid for Knudsen numbers $\mathrm{Kn} \ll 1$, which is the case in the present experiments. In the beginning of every uptake measurement $p_{\mathrm{HCl}}^{\infty} \gg p_{\mathrm{HCl}}^{\mathrm{vap}}$ since there is no HCl dissolved in the droplet. Thus, an uptake process which is dominated by gas phase diffusion and/or surface hindrance can be revealed by an initially linear increase of the molecular number density with time, since the term on the right-hand side of eq 5 is constant if one neglects small changes in r_0. The accommodation coefficient α can be determined form the observed uptake velocity if $D_{\mathrm{HCl}}^{\mathrm{gas}}$ and $p_{\mathrm{HCl}}^{\infty}$ are known.

If the uptake process is controlled by liquid-phase diffusion inside the droplet, the temporal behavior of $\bar{n}_{\mathrm{HCl}}^{\mathrm{liq}}$ follows a multiexponential growth curve. It is then described by eq 7, which is the solution of Ficks 2nd law of diffusion for spherical geometry[15]

$$\bar{n}_{\mathrm{HCl}}^{\mathrm{liq}}(t) = n_{\mathrm{HCl}}^{\mathrm{surf}}\left[1 - \frac{6}{\pi^2}\sum_{y=1}^{\infty}\frac{1}{y^2}\exp\left(-\frac{D_{\mathrm{HCl}}^{\mathrm{liq}}y^2\pi^2}{r_0^2}t\right)\right] \tag{7}$$

Here, $n_{\mathrm{HCl}}^{\mathrm{surf}}$ is the molecular number density of HCl beneath the surface, $\mathrm{D}_{\mathrm{HCl}}^{\mathrm{liq}}$ is the diffusion coefficient of HCl in the liquid, and $\bar{n}_{\mathrm{HCl}}^{\mathrm{liq}}(t)$ is the molecular number density of HCl, averaged over the droplet volume. In contrast to the conditions that are described by eq 5, one expects that $\bar{n}_{\mathrm{HCl}}^{\mathrm{liq}}(t)$ exhibits an infinite slope at time zero.

The present results suggest that both cases are observed: Figure 6 shows the relative time-dependent increase of HCl concentration for three different H_2SO_4 concentrations at a temperature of T =189 K. The HCl concentration is given relative to its saturation value for better comparison. The shapes of these uptake curves show a smooth transition from the gas-phase diffusion or phase-passage-limited case to the liquid-diffusion-limited case. For 30 wt % sulfuric acid, the increase of HCl molecule number density is almost linear with time. The curves show saturation when the droplet approaches thermodynamic equilibrium ($p_{\mathrm{HCl}}^{\mathrm{vap}} = p_{\mathrm{HCl}}^{\infty}$ in eq 5). For 56 wt % sulfuric acid, the entire shape of the uptake curve is well described by eq 7, whereas the 40 wt % H_2SO_4 uptake curve represents an intermediate between the two different uptake dynamics. The change in uptake dynamics is due to the temperature dependence of the viscosity of aqueous H_2SO_4 solutions. At high viscosity, corresponding to low temperature and high sulfuric acid concentration, the uptake process is limited by liquid-phase diffusion. In contrast, at low viscosity i.e., high temperature and low sulfuric acid concentration, the process is dominated by gas-phase diffusion and/or the phase passage. This is summarized in Figure 7, where the two distinct regions are shown as a function of temperature and concentration. These two regimes are analyzed in sections B and C.

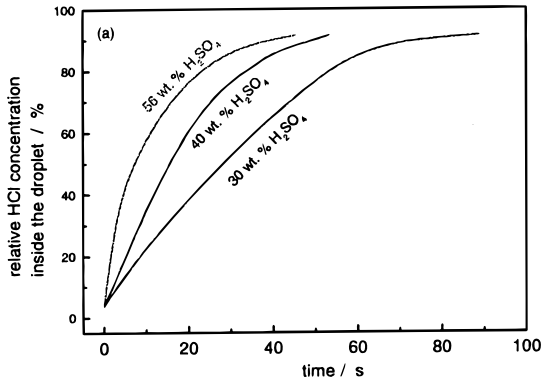

Figure 6. HCl uptake curves for three different H_2SO_4 concentrations at T = 189 K.

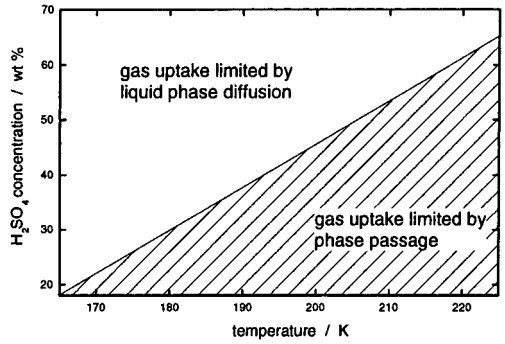

Figure 7. Experimentally observed regions of different uptake dynamics as a function of temperature and H_2SO_4 concentration.

The gas uptake is measured until saturation is reached, to deduce directly D^{liq} by fitting eq 7 to our data. It is important to note that only the relative increase $\bar{n}_{\mathrm{HCl}}^{\mathrm{liq}}(t)/n_{\mathrm{HCl}}^{\mathrm{surf}}$ of the HCl concentration has to be known in order to determine D^{liq}. Therefore, any uncertainty in the HCl partial pressure in the trap chamber does not affect the determination of D^{liq}. The D^{liq} value is measured directly in the present experiments, which is different from experiments in coated wall flow tubes where usually the product of D^{liq} and H^*, the effective Henry constant, is determined. Independent measurements of H^* are then needed in order to obtain D^{liq}.

B. Liquid-Phase Diffusion. Figure 8 shows HCl uptake curves of 48 wt % H_2SO_4 recorded at four different tempera-

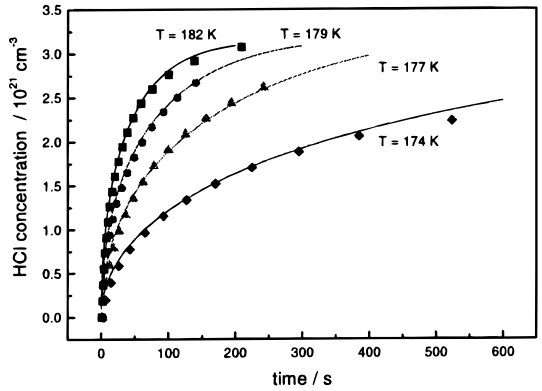

Figure 8. Measured increase of HCl molecular number density inside 48 wt % H_2SO_4 droplets at different temperatures. The symbols correspond to the appearance of Mie resonances during the HCl uptake.

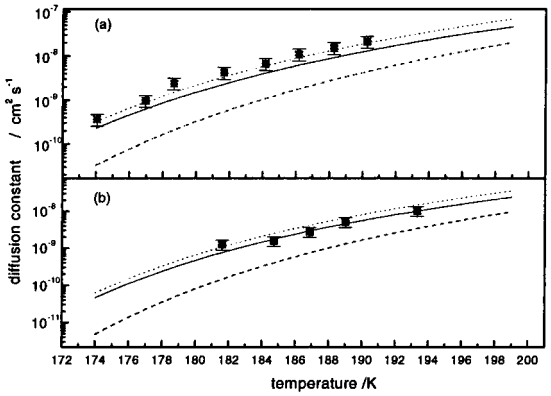

Figure 9. Measured liquid diffusion constants at two different H_2SO_4 concentrations (a) 48 wt % and (b) 56 wt % as a function of temperature. Dashed lines: Theoretical calculations for the same concentrations using the cubic cell model from ref 34 assuming that Cl^- is the diffusing species. Solid line: Hayduk/Minhas parameter-free model from ref 31. Dotted line $D^{liq} = CT/\eta^{0.83}$ with C from ref 6. For details see text.

tures. Each measurement was carried out at a constant HCl partial pressure of 1.2×10^{-4} bar. The symbols correspond to the occurrence of Mie resonances (see Figure 4). The solid lines are fits to the experimental data using eq 7 with D^{liq} and n_{HCl}^{surf} as the only free parameters. As one expects, the uptake velocity decreases with falling temperature. Figure 9 shows the experimental liquid diffusion constants of HCl in H_2SO_4/H_2O droplets in the 174−194 K temperature regime (full squares, Figure 9a: 48 wt % H_2SO_4, Figure 9b: 56 wt % H_2SO_4). The good agreement between experiment and fit allows to obtain D^{liq} with high accuracy. Similar curves were obtained for 56 wt % H_2SO_4 solution droplets in a temperature range between $T = 180$ and 193 K.

In atmospheric modeling D^{liq} is usually derived from liquid viscosity data (see for example ref 22). The most widely known dependence between D^{liq} and η is the Stokes−Einstein relation

$$D^{liq} = CT/\eta \tag{8}$$

Various empirical parameterizations[12] of the constant C in eq 8 have been made as a function of the effective length scales of solute and solvent. These models assume that a relatively large molecule diffuses in a solvent of comparably small or at least similarly sized molecules. In highly viscous solvents, however, one may question if this assumption is still valid. In the present work, it is rather a small solute molecule, diffusing in a solvent of larger molecules. A breakdown of the Stokes−Einstein relation in highly viscous liquids has been observed in[23−28] and was attributed to structure building of the solvent molecules. It is assumed that the motion of a molecule, diffusing through different structural domains, will not depend as strongly on the viscosity of the solvent as predicted from the Stokes−Einstein relation. Therefore, for viscous solvents a dependence of the form

$$D^{liq} = CT/\eta^q \tag{9}$$

has been suggested where the constants C and q are specific for a given solute and solvent (e.g., polar or nonpolar)[12] and q varies between 0.5 and 1. This was promoted by measurements of Hiss and Cussler,[25] who suggested $q = 2/3$ for organic solvents if the viscosity exceeds 5 cP, Fujara et al.,[26] who determined $q = 0.75$ for self-diffusion in orthoterphenyl at temperatures close to the glass transition, and Langenberg et al.,[29] who found $q = 0.88$ for several atmospheric trace gases in sulfuric acid solutions at $T = 203-243$ K, respectively.

Another empirical correlation between diffusion coefficient and viscosity is given by Hayduk and Minhas.[12,30] They propose for a solute A dissolved in an aqueous solution B the following dependence:

$$D_{AB} = 1.25 \times 10^{-8}(V_A^{-0.19} - 0.292)\, T^{1.52}\, \eta^{(9.58/V_A - 1.12)} \tag{10}$$

Here, V_A, given in units of cm^3/mol, is the molar volume of the solute A at its normal boiling temperature. It accounts for the dependence of the diffusion coefficient on the size of the diffusing molecules. Viscosity data of supercooled H_2SO_4/H_2O solutions are reported in the literature.[31] The analytic expression for the temperature dependence of the viscosity η[32] can be used for extrapolation down to $T < 200$ K. On this basis we calculate D^{liq} of HCl according to the three models mentioned above. In Figure 9a and 9b, the dashed lines represent the cubic cell model (CCM),[33] which is Stokes−Einstein type (eq 8) and which was used earlier by Luo et al.[22] The CCM describes the overall temperature trend of the present data but lies consistently about a factor of 6 below the experimental values. Thus, the Stokes−Einstein relation can only fit our results if an unrealistically small diameter of the solute is assumed. However, the CCM was successfully used by Klassen et al.[6] to describe D_{HCl}^{liq} at higher temperatures. They note that this approach does not work so well for HBr.

The solid lines in Figure 9 were calculated according to eq 10 with $V_A = 30.8$ cm^3/mol[34]. Taking into account that this model contains no adjustable parameter, it represents the experimental data remarkably well. The dotted lines in Figure 9 have been obtained from eq 9. Here $C = 7.8$ cm^2 cP/sK from ref 6 was used, and q was the only adjustable parameter. We obtain good agreement with the experimental results for $q = 0.83$. This compares well with previous results of Langenberg et al.[29] who found $q = 0.88$ for the diffusion of several trace gases in H_2SO_4 solutions at slightly higher temperatures.

Recently, diffusion constants of HCl in H_2SO_4 solutions at higher temperatures have been measured by Klassen et al.[6] Their results are included in Figure 10 together with our data and the curves from eq 10 for the H_2SO_4 concentrations used in both experiments. Though both experiments use different experimental techniques to determine D_{HCl}^{liq} and span a large temperature range, they are described by the model of Hayduk and Minhas without the need for any adjustable parameter. Using V_A of HBr from ref 34, the same model also gives good agreement with D_{HBr}^{liq} from ref 6 (not shown in Figure 10).

Conversely, an extrapolation of our fit using eq 9 (dotted lines in Figure 9) to higher temperatures does not agree well

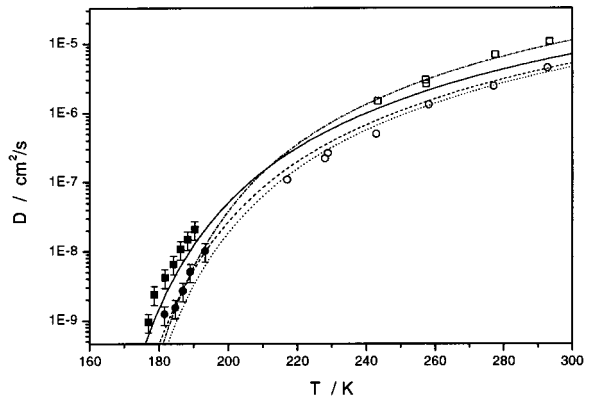

Figure 10. Liquid diffusion constants for H_2SO_4 solutions as a function of temperature (solid squares 48 wt % and circles 56 wt %, this work). Open circles and squares: Measured liquid diffusion constants for two different H_2SO_4 concentrations (30 wt % and 60 wt %) from ref 6. Lines: theoretical calculations using the Hayduk/Minhas parameter-free model[31]. Solid line: 60 wt % H_2SO_4. Dashed line: 56 wt % H_2SO_4. Dotted line: 48 wt % H_2SO_4. Dash dotted line: 30 wt % H_2SO_4.

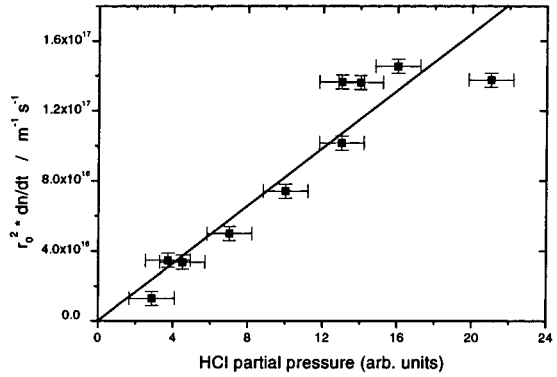

Figure 11. Initial uptake velocity of 40 wt % sulfuric acid as a function of the relative HCl partial pressure outside the trap chamber as measured by a quadrupole mass spectrometer.

with the data reported in ref 6. Nevertheless, this can be rationalized by a smooth transition from eq 9 to the Stokes−Einstein relation with increasing temperature.

C. Accommodation Kinetics. The accommodation coefficient α can be determined under conditions where liquid diffusion plays no role in the uptake process by using eqs 5 and 6 (cf. Figure 7). We measured the uptake velocity of numerous droplets as a function of the HCl partial pressure at constant temperature in order to verify the validity of eq 5. The dn_{HCl}^{liq}/dt value is determined by evaluating only the first 3−4 MDR resonances of the droplet in order to be sure that $p_{HCl}^{\infty} \approx (p_{HCl}^{\infty} - p_{HCl}^{vap})$. The p_{HCl}^{∞} value is assumed to be a linear function of the HCl^+ mass signal at $m/z = 36$ that is recorded by the quadropole mass spectrometer. Since α should not vary with the HCl partial pressure, a $r_0^2 \cdot dn_{HCl}^{liq}/dt$ versus p_{HCl}^{∞} plot is expected to exhibit a linear behavior that should also contain the origin, as shown in Figure 11. We plot $r_0^2 \cdot dn_{HCl}^{liq}/dt$ against the HCl^+ signal, since the initial droplet radius is slightly different for each measurement. Each data point in Figure 11 corresponds to an uptake measurement of a single droplet. We note that in the regime where the phase passage limits the uptake rate (Figure 7), the expected linear relationship is always observed. This proofs, that the transport of HCl toward the droplet is indeed governed by gas phase diffusion. Right after droplet injection, the gas phase around the droplet becomes radially HCl depleted and a steady-state pressure profile is established in the microsecond time regime.[19] By calculating D^* from the experimental data for every droplet, accommodation coefficients α can be determined using eqs 5 and 6. The HCl gas-phase diffusion coefficient can be estimated according to refs 11 and 20. We find accommodation coefficients of the order of 10^{-2} (30−40 wt % H_2SO_4, $T = 185-207$ K), thus being significantly lower than those reported in ref 9b.

Experimentally, there is evidence for HCl depletion in the gas mixture when the N_2/HCl mixture enters the trap chamber (cf. section II). This effect is presumably responsible for a difference in HCl partial pressure between a location close to the droplet and the location where it is actually measured by the QMS. Therefore, we assume that, in our experiment, p_{HCl} close to the droplet is lower than the value obtained from the calibrated QMS signal. This would lead to α values that are too low. To overcome the systematic error in the determination of p_{HCl}^{∞}, additional work is in progress to measure p_{HCl}^{∞} close to the droplet by spectroscopic approaches.

IV. Conclusion

The HCl uptake dynamics of supercooled sulfuric acid solution droplets has been investigated using the technique of single-particle levitation. The gas uptake dynamics is observed as a function of temperature, sulfuric acid concentration, and the gas phase partial pressure of HCl. The kinetics depends strongly on the viscosity of the H_2SO_4 solution. At stratospheric temperatures, the uptake dynamics change from the phase-passage-limited to the liquid-diffusion-limited case with increasing viscosity of the droplet.

Diffusion constants of HCl inside a supercooled H_2SO_4 have been determined by analyzing the experimental uptake curves with the Ficks 2nd law of diffusion for spherical geometry. The measurements have been carried out at temperatures between 180 and 194 K for 56 wt. % H_2SO_4 and between 174 and 190 K for 48 wt % H_2SO_4 solutions. The results confirm that, in the case of small solutes such as HCl diffusing through a liquid environment of larger molecules, the diffusion coefficient is no longer inversely proportional to the viscosity of the solution. Extrapolating diffusion data with Stokes−Einstein type models to stratospheric temperatures will yield diffusion constants that are too low. The parameter-free model of Hayduk and Minhas[30] represents both our data on D^{liq} and the data of Klassen et al.[6] remarkably well. This good accordance suggests, that extrapolation of viscosity data using the equation proposed in ref 32 yields good results down to 174 K. We further note that the relation $D = C/\eta^{0.83}$ can be applied for the diffusion of HCl in supercooled sulfuric acid solutions below 200 K.

In regimes, where gas-phase diffusion with subsequent accommodation/dissolution at the liquid surface limits the uptake (30−40 wt % H_2SO_4, 183−207 K), a linear dependence between uptake velocity and HCl partial pressure p_{HCl} is observed indicating that the uptake is governed by diffusion and subsequent surface accommodation. The obtained uptake velocities can be further analyzed[20] to deduce accommodation coefficients. However, demixing of the gas mixture at low temperatures inside the reaction chamber has likely obstructed the quantitative evaluation of the uptake curves. Nevertheless, we propose this method after suitable improvements of p_{HCl} measurements close to the droplet, to determine α of stratospherically relevant trace gases such as HNO_3 and $ClONO_2$ on supercooled solutions.

Acknowledgment. The authors thank T. Koop, S. Meilinger, and U. Krieger for helpful discussions. Financial support is gratefully acknowledged by the Kommission für Forschung und

Nachwuchs (FNK) of the Freie Universität Berlin and the Fonds der Chemischen Industrie.

References and Notes

(1) (a) Tolbert, M. A. *Science* **1994**, *264*, 527. (b) MacKenzie, A. R.; Kulmala, M.; Laaksonen, A.; Vesala, T. *J. Geophys. Res.* **1995**, *100*, 11275. (c) Koop, T.; Carlslaw, K. *Science* **1996**, *272*, 1638.

(2) Peter, T. *Annu. Rev. Phys. Chem.* **1997**, *48*, 785.

(3) Ravishankara, A. R.; Hanson, D. R. *J. Geophys. Res.* **1996**, *101*, 3885.

(4) McElroy, M. B.; Salawitch, R. J.; Wofsy, S. C.; Logan, J. A. *Nature* **1986**, *321*, 759.

(5) Carslaw, K. S.; Wirth, M.; Tsias, A.; Luo, B. P.; Dörnbrack, A.; Leutbecher, M.; Volkert, H.; Renger, W.; Bacmeister, J. T.; Peter, T. *Nature* **1998**, *391*, 675.

(6) Klassen, J. K.; Hu, Z.; Williams, L. R. *J. Geophys. Res.* **1998**, *103*, 16197.

(7) Kolb, C. E.; Worsnop, D. R.; Zahniser, M. S.; Davidovits, P.; Keyser, L. F. In *Progress and Problems Atmospheric Chemistry*; Barker, J. R., Ed.; World Scientific: Singapore, 1995.

(8) (a) Williams, L. R.; Golden, D. M. *Geophys. Res. Lett.* **1993**, *20*, 2227. (b) Tolbert, M. A.; Rossi, M. J.; Golden, D. M. *Geophys. Res. Lett.* **1988**, *15*, 847.

(9) (a) van Doren, J. M.; Watson, L. R.; Davidovits, P.; Worsnop, D. R.; Zahniser, M. S.; Kolb, C. E. *J. Phys. Chem.* **1990**, *94*, 3265. (b) Robinson, G. N.; Worsnop, D. R.; Jayne, J. T.; Kolb, C. E.; Swarz, E.; Davidovits, P. *J. Geophys. Res.* **1988**, *103*, 25371.

(10) Hanson, D. R.; Ravishankara, A. R. *J. Phys. Chem.* **1993**, *97*, 12309.

(11) Davis, E. J. *Aerosol Sci. Technol.* **1997**, *26*, 212.

(12) Reid, R. C.; Prausnitz, J. M.; Poling B. E. *The Properties of Gases and Liquids*, McGraw-Hill: New York, 1987; Chapter 11.

(13) Krämer, B.; Schwell, M.; Hübner, O.; Vortisch, H.; Rühl, E.; Baumgärtel, H.; Wöste, L.; Leisner, T. *J. Chem. Phys.* **1999**, *111*, 6521.

(14) (a) Paul, W.; Raether, M. *Z. Phys.* **1955**, *140*, 262. (b) Fischer, E., *Z. Phys.* **1959**, *156*, 1.

(15) Carslaw, H. S.; Jaeger, J. C. *Conduction of Heat in Solids*; Clarendon Press: Oxford, 1959.

(16) Krämer, B.; Schwell, M.; Hübner, O.; Vortisch, H.; Leisner, T.; Rühl, E.; Baumgärtel, H.; Wöste, L. *Ber. Bunsen-Ges. Phys. Chem.* **1996**, *100*, 1911.

(17) Bohren, C. F.; Huffmann, D. R. *Absorption and Scattering of Light by Small Particles*; Wiley: New York, 1983.

(18) Steiner, B.; Berge, B.; Gausmann, R.; Rohmann, J.; Rühl, E. *Appl. Opt.* **1999**, *38*, 1523.

(19) Schwartz, S. E. In *Chemistry of Multiphase Atmospheric Systems*; Jaeschke, W., Ed.; NATO ASI Series, Springer: Berlin, 1986.

(20) Meilinger, S. *Non-equilibrium Liquid Stratospheric Aerosols*, Diploma thesis, Universität Mainz, **1995**.

(21) (a) Hertz, H. *Ann. Phys.* **1882**, *17*, 177. (b) Knudsen, M., *Ann. Phys.* **1915**, *47*, 697.

(22) Luo, B. P.; Clegg, S. L.; Peter, T.; Müller, R.; Crutzen, P. J. *Geophys. Res. Lett.* **1994**, *21*, 49.

(23) Tarjus, G.; Kivelson, D. *J. Phys. Chem.*, **1995**, *103* (8), 3071.

(24) Hayduk, W.; Cheng, S. C. *Chem. Eng. Sci.* **1971**, *26*, 635.

(25) Hiss, T. G.; Cussler, E. L. *AIChE J.* **1973**, *19* (4), 698.

(26) Fujara, F.; Geill, B.; Sillescu, H.; Fleischer, G. *Z. Phys. B* **1992**, *88*, 195.

(27) Chang, I.; Fujara, F.; Geil, B.; Heuberger, G.; Mangel, T.; Sillescu, H. *J. Non-Cryst. Solids* **1994**, *248*, 172.

(28) Heuberger, G.; Sillescu, H. *J. Phys. Chem.* **1996**, *100*, 15255.

(29) Langenberg, S.; Proksch, V.; Schurath, U. *Atmos. Environ.* **1998**, *32* (19), 3129.

(30) Hayduk, W.; Minhas, B. S. *Can. J. Chem. Eng.* **1982**, *60*, 295.

(31) Williams, L. R.; Long, F. S. *J. Phys. Chem.* **1995**, *99*, 3748.

(32) Eicher, L. D.; Zwolinski, B. J. *J. Phys. Chem.* **1971**, *75*, 2016.

(33) Houghton, G. *J. Chem. Phys.* **1964**, *40* (6), 1628.

(34) Gmelin *Handbuch der anorganischen Chemie*, 8. Aufl.; VCH: Weinheim, 1960.